in $CD_3OD$ and DMSO-$d_6$ solution, consistent with dissociation (eq 1).

$$Fe_2(H_2O)(O_2CR)_4(tmen)_2 \rightarrow 2Fe(O_2CR)_2(tmen) + H_2O \quad (1)$$

The solid-state structures of **1** and **2** were confirmed by single-crystal X-ray determinations (**2** is shown in Figure 1 and **1** in Figure S-I in the supplementary material). Each complex consists of a $\mu$-aqua bis($\mu$-$O_2CR$) diiron core with additional terminal carboxylate ligands coordinated to each Fe and arranged such that the uncoordinated oxygens O(7) and O(9) are involved in strong hydrogen bonding with the bridging water [O(1)···O(7), 2.57 Å in **1** and 2.54 Å in **2**; O(1)···O(9), 2.58 Å in **1** and 2.57 Å in **2**]. This results in a twisting of the bridging water oxygen away from a tetrahedral geometry as reflected in Fe–O–H angles [in **2**: Fe(1)–O(1)–H(1A), 126.3 (3)°; Fe(2)–O(1)–H(1B), 118.4 (2)°; Fe(1)–O(1)–H(1B), 97.0 (2)°; Fe(2)–O(1)–H(1A), 95.6 (2)°; but H(1A)–O(1)–H(1B), 108.7 (3)°]. The hydrogen bonds in **2** are symmetric [O(1)–H(1A), 1.08 Å; O(1)–H(1B), 0.98 Å], but in **1** they are asymmetric [O(1)–H(1A), 0.85 Å; O(1)–H(1B), 1.37 Å]. Fe–O bond lengths for oxygens trans to the terminal carboxylates are considerably shorter than those trans to the nitrogen donors in **1**, but not in **2**. The Fe···Fe separations and the Fe–($\mu$-O) bonds are considerably larger than those found in diiron(II) complexes with bridging $OH^-$, $[Fe_2(OH)(O_2CCH_3)_2(Me_3TACN)_2]^+$ (3.32 Å),[6] $OR^-$, $[Fe_2BPMP(O_2CCH_2CH_3)_2]^+$ (3.348 Å),[15] $[Fe_2(N\text{-}Et\text{-}HPTB)(O_2CPh)_2]^{2+}$ (3.473 Å),[16] or O,OCHO$^-$, $[Fe_2(BIPhMe)_2(HCO_2)_4]$ (3.585 Å),[17] which is consistent with a neutral bridging ligand.

The Mössbauer spectra confirm the high-spin iron(II) oxidation state.[18] Only one doublet is observed for **2**, but the appearance of two resolvable doublets for **1** indicates that the structural asymmetry is reflected in slightly different electronic environments for the two iron atoms. These values are very similar to a fit of the spectrum of the diiron(II) form of RRB2 from *Escherichia coli*.[19]

Preliminary magnetic susceptibility measurements on powdered samples and frozen solutions of **1** and **2** indicate substantially weaker magnetic coupling between iron atoms than is observed for $OH^-$-bridged **3**[6d] ($J = -13.1$ cm$^{-1}$) and deoxyhemerythrin ($J = -12$ to $-38$ cm$^{-1}$ by MCD-ESR,[4] and $-15$ cm$^{-1}$ by $^1$H NMR[20]). This decreased coupling in **1** and **2** is consistent with the weakly ferromagnetic behavior found in deoxyHr$N_3$.[4] Complexes **1** and **2** are EPR silent,[21] in contrast to deoxyHr$N_3$, which exhibits a low-field EPR signal.[4,22] However, either type of EPR behavior is consistent with an integer-spin ground state.[15b,23,24]

In conclusion, the first examples of diiron(II) complexes containing a bridging water have been prepared. The structure of **2** has been shown by $^1$H NMR to be maintained in noncoordinating aprotic solvents, but not in protic or strongly coordinating solvents. Protonation of the bridging oxygen results in the longest Fe(II)···Fe(II) and Fe–$O_{bridge}$ distances yet observed in similar tribridged structures. These longer distances are reflected in considerably weaker intramolecular magnetic interactions in complexes **1** and **2** compared to analogous hydroxo-bridged complexes. The magnetic interactions in **1** and **2** resemble the weakly ferromagnetic interactions observed in the diiron(II) forms of deoxyHr$N_3$, MMO, and RRB2.

**Acknowledgment.** We thank Dr. N. Ravi and Professor B. H. Huynh for Mössbauer data, R. Reagan, Dr. P. Wang, Dr. S. Nimmala, and Professor E. P. Day for magnetic data, and Dr. M. P. Hendrich for EPR spectra. This research was supported in part by the University Research Committee of Emory University, the donors of the Petroleum Research Fund, administered by the American Chemical Society, and the National Institutes of Health (GM 46506).

**Supplementary Material Available:** Magnetic susceptibility plots for **2**, an ORTEP drawing of **1**, and tables of atomic positional and thermal parameters and bond lengths and angles of **1** and **2** (23 pages); observed and calculated structure factors for **1** and **2** (10 pages). Ordering information is given on any current masthead page.

(15) (a) Borovik, A. S.; Que, L., Jr. *J. Am. Chem. Soc.* **1988**, *110*, 2345–2347. (b) Borovik, A. S.; Hendrich, M. P.; Holman, T. R.; Münck, E.; Papaefthymoiu, V.; Que, L., Jr. *J. Am. Chem. Soc.* **1990**, *112*, 6031–6038.
(16) Menage, S.; Brennan, B. A.; Juarez-Garcia, C.; Münck, E.; Que, L., Jr. *J. Am. Chem. Soc.* **1990**, *112*, 6425–6426.
(17) (a) Tolman, W. B.; Bino, A.; Lippard, S. J. *J. Am. Chem. Soc.* **1989**, *111*, 8522–8523. (b) Tolman, W. B.; Liu, S.; Bentsen, J. G.; Lippard, S. J. *J. Am. Chem. Soc.* **1991**, *113*, 152–164.
(18) For measurements made at 4.2 K and referenced to iron metal at room temperature: for **1**, $\Delta E_Q(1) = 3.11$, $\delta(1) = 1.25$, and $\Delta E_Q(2) = 2.70$, $\delta(2) = 1.26$; for **2**, $\Delta E_Q = 2.75$, $\delta = 1.27$ mm/s.
(19) $\Delta E_Q(1) = 3.28$ mm/s, $\delta(1) = 1.27$ mm/s, and $\Delta E_Q(2) = 2.93$ mm/s, $\delta(2) = 1.26$ mm/s. Lynch, J. B.; Juarez-Garcia, C.; Münck, E.; Que, L., Jr. *J. Biol. Chem.* **1989**, *264*, 8091–8096.
(20) Maroney, M. J.; Kurtz, D. M., Jr.; Nocek, J. M.; Pearce, L. L.; Que, L., Jr. *J. Am. Chem. Soc.* **1986**, *108*, 6871–6879.
(21) Spectra of frozen (<10 K) acetonitrile and chloroform solutions run with the microwave field both perpendicular and parallel to the static magnetic field.
(22) Hendrich, M. P.; Pearce, L. L.; Que, L., Jr.; Chasteen, N. D.; Day, E. P. *J. Am. Chem. Soc.* **1991**, *113*, 3039–3044.
(23) (a) Hendrich, M. P.; Debrunner, P. G. *Biophys. J.* **1989**, *56*, 489–506. (b) Hendrich, M. P.; Debrunner, P. G. *J. Magn. Reson.* **1988**, *78*, 133–141.
(24) Dexheimer, S. L.; Gohdes, J. W.; Chan, M. K.; Hagen, K. S.; Armstrong, W. H.; Klein, M. P. *J. Am. Chem. Soc.* **1989**, *111*, 8923–8925.

## Catalytic Mechanism of Cytochrome P-450: Evidence for a Distal Charge Relay

Nancy C. Gerber and Stephen G. Sligar*

*Departments of Biochemistry, Chemistry and Biophysics and The Beckman Institute for Advanced Science and Technology, University of Illinois Urbana, Illinois 61801*

*Received June 22, 1992*

The cytochromes P-450 are responsible for a plethora of critical biotransformations in humans, animals, microbes, insects, and plants.[1-6] They have received considerable attention from mechanistic chemists due to the enzyme's ability to catalytically oxygenate recalcitrant substrates with controlled regiospecificity and stereochemistry. The oxygenase cycle of cytochrome P-450 involves sequential substrate binding, ferric–ferrous reduction of the heme active center, and dioxygen association to form a ternary complex analogous to the oxygenated forms of hemoglobin and myoglobin. Subsequent steps are less well understood, but can be hypothetically visualized as input of a second reducing equivalent, heterolytic scission of the O–O bond releasing water, and formation of a transient metal–oxo complex that is two oxidation equivalents above the ferric resting state, analogous to compound I in the peroxidases.[7] Completion of the oxygenase cycle involves hydrogen abstraction from the substrate and "oxygen rebound"[8,9] with product release, regenerating the ferric resting state.

To date, the only published X-ray structures of a cytochrome P-450 are that of P-450$_{cam}$ (P450101), active in the hydroxylation of camphor in *Pseudomonas*.[10] The crystal structure of cytochrome *c* peroxidase (CCP)[11] provided a strong suggestion as to

(1) Sligar, S. G.; Filipovic, D.; Stayton, P. S. In *Methods in Enzymology*; Waterman, M. R., Johnson, E. F., Eds.; Academic Press: New York, 1992; Vol. 206, pp 31–49.
(2) Murray, R. I.; Sligar, S. G. In *Cytochrome P-450: Structure, Mechanism, and Biochemistry*; Ortiz de Montellano, P. R., Ed.; Plenum Press: New York, 1986; pp 429–503.
(3) White, R. E.; Sligar, S. G.; Coon, M. J. *Modes of Oxygen Activation by Cytochrome P-450*; Elsevier/North-Holland Biomedical Press: Amsterdam, 1980; pp 307–310.
(4) Dawson, J. H. *Science* **1988**, *240*, 433–439.
(5) Guengerich, F. P. *Asia Pac. J. Pharmacol.* **1990**, *5*, 253–268.
(6) Johnson, E. F. *TiPS* **1992**, *13*, 122–126.
(7) Coulson, A. F.; Erman, J. E.; Yonetani, T. *J. Biol. Chem.* **1971**, *246*, 917–924.
(8) Groves, J. T.; McCluskey, G. A.; White, R. E.; Coon, M. J. *Biochem. Biophys. Res. Commun.* **1978**, *81*, 154–160.
(9) Groves, J. T.; McCluskey, G. A. *J. Am. Chem. Soc.* **1976**, *98*, 859–861.
(10) Poulos, T. L.; Raag, R. *FASEB* **1992**, *6*, 674–679.
(11) Poulos, T. L.; Finzel, B. C. In *Peptide and Protein Reviews*; Hearn, M. T. W., Ed.; Marcel Dekker, Inc.: New York, 1984; Vol. IV, pp 115–171.

0002-7863/92/1514-8742$03.00/0 

**Table I.** Kinetic and Thermodynamic Parameters of Cytochrome P-450$_{cam}$

| assay | wt | D251N |
|---|---|---|
| substrate binding[a] | | |
| $k_{on}$, $\mu M^{-1}$ $s^{-1}$ | 24.5 | 22.4 |
| $k_{off}$, $s^{-1}$ | 21.1 | 15.0 |
| $K_d$, $\mu M$ | 0.86 | 0.67 |
| first electron transfer[a] | | |
| $k_{obsd}$, $s^{-1}$ | 60.7 | 145.2 |
| oxygen binding[b] | | |
| $k_{on}$, $\mu M^{-1}$ $s^{-1}$ | 81.0 | 56.0 |
| $k_{off}$, $s^{-1}$ | 2.65 | 2.93 |
| autooxidn[c] | | |
| $k_{obsd}$, $s^{-1}$ | 0.0041 | 0.0027 |
| NADH oxidn rate,[d] $\mu M/min/\mu M$ heme | 847 | 8 |
| 5-OH[20]/NADH | 0.95 | 0.14 |
| NADH/$O_2$ | 1.03 | 1.40 |

[a] 20 °C in 50 mM KPi, pH 7.2, methods as in refs 19 and 20. [b] 15 °C in 50 mM KPi, pH 7.2. [c] Methods as in ref 14. [d] 50 mM Tris Cl, pH 7.4, 0.1 M KCl, 250 $\mu$M NADH, 2 $\mu$M Fp, 1 $\mu$M P-450, 10 $\mu$M Pd. Methods as in ref 21.

the mechanism of O–O bond scission that involved acid–base catalysis by arginine and histidine in the distal pocket. That these residues were not found in the P-450 active site prompted the suggestion that only the proximal cysteine ligand was required for O–O bond scission.[4] Two polar groups, however, are in the active site of P-450$_{cam}$. A hydroxyl and a carboxylate are found in close proximity in the only two crystal structures of cytochromes P-450 and are adjacent in the majority of aligned P-450 sequences (positions 252 and 251, respectively, in P-450$_{cam}$).[12] Site-directed mutagenesis has been used to show that Thr 252 functions to stabilize both the one- and two-electron reduced oxygen intermediates.[13,14] In order to ascertain the function of Asp251 in P-450$_{cam}$, we have mutated this residue to asparagine and determined all of the accessible fundamental rates and equilibria of the cycle (Table I).

The most striking effect of changing the acid function at position 251 to an amide is a drastic decrease in the catalytic turnover of the system.[15] Table I shows that this is not due to substrate binding, ferric–ferrous reduction of the heme iron, or dioxygen binding. Rather, the reduction in NADH oxidation kinetics is due to the coupled second electron transfer and oxygen activation step as evidenced in a single turnover stopped flow experiment mixing equimolar amounts of reduced P-450 and putidaredoxin with oxygenated buffer ($t_{1/2}$ = 20 ms, wt, and $t_{1/2}$ > 70 s, D251N). Additionally, Table I illustrates that redox input into the P-450 hemoprotein is no longer completely coupled to substrate hydroxylation. Electron equivalents are now appearing as hydrogen peroxide and water.

An enzyme mechanism consistent with these results is shown in Figure 1. Thr252 forms a hydrogen bond to the bound dioxygen and stabilizes this state and the peroxo complex as previously suggested.[10,13,14] Although the crystal structure of P-450$_{cam}$ has this side chain in a different rotamer configuration (hydrogen bonded to the backbone of Gly248 at the site of a kink in the I helix), dynamics simulations and the crystal structure of the Thr252Ala mutant show this region to be highly mobile.[16,17] We

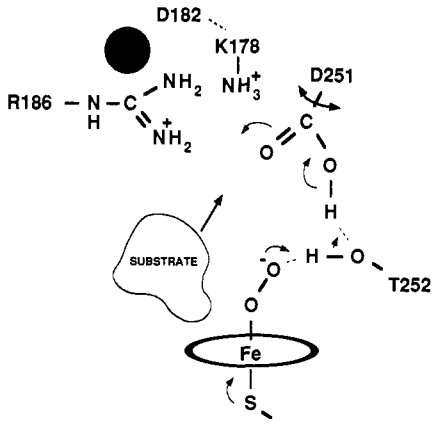


**Figure 1.**

have modeled a bound dioxygen into the P-450$_{cam}$ crystal structure and found that rotation about the Thr252 $C_\alpha$–$C_\beta$ bond brings the hydroxyl hydrogen within 1.85 Å of the distal oxygen of $O_2$. Asp251 is seen to be hydrogen bonded to Arg186 and Lys178 in the crystal structure, yet can adopt the rotamer configuration shown in Figure 1. We propose that (Asp182-Lys178,Arg186)-Asp251-Thr252 forms a charge relay system in the distal pocket of P-450. In this model, Asp251 serves as a proton shuttle between the solvent-accessible Asp182-Lys178,Arg186 network and Thr252. In addition to providing a proton conduit, the configuration shown in Figure 1 provides a general-acid-catalytic mechanism that should aid cleavage of the oxygen–oxygen bond in the iron-bound complex. This model explains the partitioning of reducing equivalents in wild-type, Thr252, and Asp251 mutants of P-450$_{cam}$. Without the Thr252 hydroxyl, rapid autooxidation reactions ensue that release superoxide and peroxide with very little substrate hydroxylation. Hence the committed step of oxygen–oxygen bond scission needs a general-acid assist. Replacing Asp251 with Asn alters the basisity of Thr252 such that catalysis is drastically slowed. Replacement of Asp251 with Gly or Ala essentially abolishes activity, and mutations of Arg186 and Lys178 also decrease overall enzymatic activity.[15] A similar role for a threonine or serine hydroxyl may also operate in the cytochrome oxidases.[22] We propose that the Asp251 "shuttle" operates between two stable conformations as shown in Figure 1. The Asp251-Arg186 and Asp251-Lys178 salt bridges connect the F-G loop to the I helix, while the Asp182-Lys178 salt bridge provides the link to solvent. This F-G loop region has been proposed as part of the substrate access pathway to the buried pocket of P-450$_{cam}$.[18] As such, this salt linkage could couple substrate access/binding to catalysis through control of substrate entry. Interestingly, in this regard, the D251N mutation drastically affects the activation enthalpy of the camphor *on* rate but does not affect the activation enthalpy for the dissociation of substrate (data not shown). It should be stressed that these experiments do not rule out a critical role for protein-bound water in delivering protons to reduced iron–oxygen intermediates[10] either through direct participation in a charge relay involving Asp251 and Thr252 or through greater solvent access following mutation at these positions.

**Acknowledgment.** This work was supported by grants from the National Institutes of Health (GM31756 and GM33775).

(12) Nelson, D. R.; Strobel, H. W. *Biochemistry* **1989**, *28*, 656–660.
(13) Imai, M.; Shimada, H.; Watanabe, Y.; Matsushima-Hibiya, Y.; Makino, R.; Koga, H.; Horiuchi, T.; Ishimura, Y. *Proc. Natl. Acad. Sci. U.S.A.* **1989**, *86*, 7823–7827.
(14) Martinis, S. A.; Atkins, W. M.; Stayton, P. S.; Sligar, S. G. *J. Am. Chem. Soc.* **1989**, *111*, 9252–9253.
(15) A preliminary report of variants of Asp251, Arg186, and Lys178 has appeared (Shimada, H.; Makino, R.; Imai, M.; Horiuchi, T.; Ishimura, Y. In *International Symposium on Oxygenases and Oxygen Activation*; Yamada Science Foundation: 1990; pp 133–136). These investigators reported that Asp251Gly and Asp251Ala displayed a marked reduction in the rate of oxygen consumption, but a very high degree of coupling of $O_2$ equivalents to product. We have generated the Asp251 to Asn, Val, and Ala mutants. The Val and Ala mutants are very unstable, and we have been unable to purify them to homogeneity.
(16) Paulsen, M. D.; Ornstein, R. L. *Proteins Struct. Funct. Genet.* **1991**, *11*, 184–204.
(17) Raag, R.; Martinis, S. A.; Sligar, S. G.; Poulos, T. L. *Biochemistry* **1991**, *30*, 11420–11429.
(18) Poulos, T. L.; Finzel, B. C.; Howard, A. J. *J. Mol. Biol.* **1987**, *195*, 687–700.
(19) Peterson, J. A. *Arch. Biochem. Biophys.* **1971**, *144*, 678–693.
(20) Pederson, T. C.; Austin, R. H.; Gunsalus, I. C. *Redox and Ligand Dynamics in P-450cam Putidaredoxin Complexes*; Pergamon Press: Oxford, 1977; pp 275–283.
(21) Atkins, W. M.; Sligar, S. G. *Biochemistry* **1988**, *27*, 1610–1616.
(22) Lemire, E.; Percy, J.; Correia, J.; Crowther, B.; Margana, F. *Current Genetics* **1991**, *20*, 121–127.
(23) Abbreviations: Pd, putidaredoxin; Fp, putidaredoxin reductase; 5-OH, 5-*exo*-hydroxycamphor.